An MTF Analysis of Papers

J. S. Arney*, Charles D. Arney, and Miako Katsube

Center for Imaging Science, Rochester Institute of Technology, Rochester, NY 14623-0887

Peter G. Engeldrum*

Imcotek Inc., Winchester, MA 01890

Resolution and tone reproduction characteristics of all hardcopy images on paper are significantly influenced by the way light scatters in the paper. However, little has been published on experimental techniques for measuring light scattering and resolution characteristics of paper. Three experimental techniques are discussed in the current work. The first is a direct measure of paper MTF by microdensitometric scans of illuminated edges projected onto the paper. This technique is tedious and of intrinsically low precision. The second technique is based on Kubelka-Munk theory and derives MTF behavior from the Kubelka-Munk equations and experimental measurements of paper reflectance. This technique has the advantage of relating paper MTF to the fundamental metrics of light scattering and light absorption. However, the accuracy of the technique is questionable due to the assumptions intrinsic to Kubelka-Munk theory. The third technique involves modeling the Yule-Nielsen effect of optical dot gain and fitting the model to experimental data. The data are generated by image analysis of idealized halftone patterns formed by placing high-resolution halftone line screens in close mechanical contact with the paper under analysis. This technique is shown to provide estimates of paper MTF with significantly higher precision than traditional microdensitometry scans of illuminated edges. Experimental data are collected for a wide variety of hardcopy substrates, and the results are used to examine some of the assumptions inherent in applying Kubelka-Munk theory to papers.

Journal of Imaging Science and Technology 40: 19–25 (1996)

Introduction

Scattering of light in paper plays a significant role in the resolution and tone reproduction characteristics of images printed on paper. In halftone images, for example, light scattering is responsible for the so called Yule–Nielsen, or optical dot gain, effect.[1,2] Light that enters a printed paper between halftone dots may scatter under a dot and be absorbed, thus causing the halftone gray scale to appear darker than intended. Electrophotographic toner particles behave somewhat like halftone dots, and the lateral scatter of light in paper has also been shown to have a major impact on electrophotographic tone reproduction.[3] Although the magnitude of the Yule–Nielsen effect is reported to depend primarily on the frequency of the halftone pattern and the magnitude of light scatter in the paper,[1,4–6] very little has been reported on techniques for measuring lateral light scattering in paper. The Yule–Nielsen n factor, an empirical constant used to model the magnitude of the Yule–Nielsen effect,[4,6] is generally considered to be an index of lateral scatter in paper. However, the n factor depends strongly on the spatial frequency of the halftone pattern and other factors.[1,7,8] Thus, while the n factor is a convenient empirical index for modeling printing processes, it is not a useful index for characterizing light scatter in paper. In the current report we would like to describe three experimental techniques for measuring lateral light scatter in papers. The relative advantages and disadvantages of these techniques will be discussed in terms of their theoretical and practical significance and in terms of their relative experimental precision.

Direct Measurements of Lateral Light Scatter

The most direct experimental technique for measuring lateral light scattering in paper was demonstrated by Yule and Nielsen in their original work on printed halftones.[4,6] A high precision "knife edge," or bar of light, can be projected onto a paper surface. With a microdensitometer one may trace the magnitude of the flux of light emerging from the paper as a function of the distance from the illuminated edge. The resulting function, LSF(x), is called the line spread function, and it provides a direct measure of the lateral distance light scatters from the illuminated edge.

A similar experiment projects a highly focused point of light onto the paper.[9,10] If the diameter of the experimental point of light is made small relative to the distance light scatters in the paper, then the decline in light flux with radial distance, x, from the illuminated point is a direct measure of the point spread function, PSF(x). The PSF and LSF are related as follows.

$$LSF(x) = \int_{-\infty}^{+\infty} PSF(x,y)\,dy. \tag{1}$$

An additional metric of lateral scatter is the modulation transfer function (MTF), defined as the modulus of the Fourier transform of the line spread function[11]:

$$MTF(\omega) = \left| \int_{-\infty}^{+\infty} LSF(x) e^{-i2\pi\omega x}\,dy \right|. \tag{2}$$

This metric describes light scatter in paper in terms of spatial frequency, ω, in units of inverse millimeters, rather than distance in millimeters.

If light is assumed to scatter the same way in all lateral directions[5] then the PSF, LSF, and MTF contain equivalent information and are often determined from the same set of data. The PSF is actually the probability density

Original manuscript received September 5, 1995.

* IS&T Members.

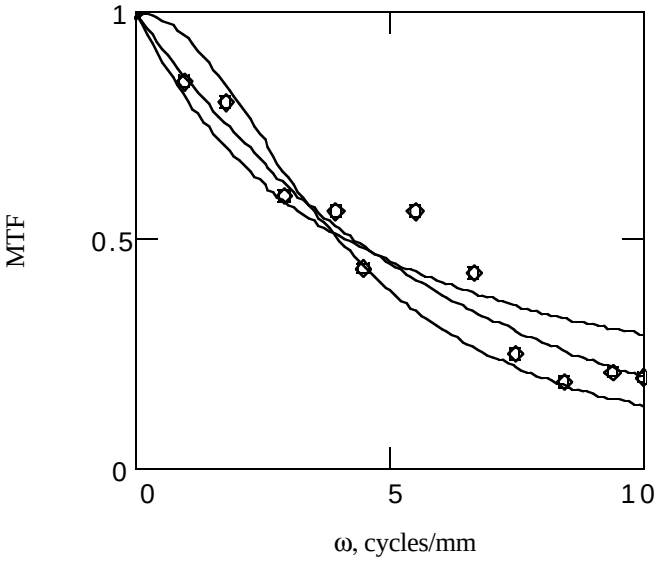

Figure 1. MTF reported by Engeldrum and Pridham[12]. Dots are calculated from an edge trace measurement, and the lines are typical MTF models, e^{-kx} and $[1 + (k\omega)^m]^{-1}$ with m = 1 and 2.

function for a photon emerging a distance, x, from its point of entry in the paper. The MTF, on the other hand, is a more practical metric for describing resolution characteristics of an imaging system, since a system MTF is the mathematical product of the MTFs of the components of the system (lens, emulsion, paper, etc.) The LSF is a less important metric but is more easily measured experimentally, and so MTF and PSF are often inferred from experimental microdensitometric measurements of the LSF. Figure 1 illustrates an MTF calculated point by point from an edge trace experiment reported previously[12] for a typical noncoated copy paper. The noise typical of edge trace experiments makes it difficult to determine empirically the type of function that best describes lateral light scattering in paper. As an example, three functions commonly used to model MTF curves[11] are shown as solid lines in Fig. 1, and it is clear the data do not really fit one function significantly better than another.

Yule and Nielsen suggested that the LSF characteristic of paper is Gaussian.[4] The corresponding MTF is also a Gaussian function.[11] However, other reports suggest that the PSF is an exponential function,[10] which would make the LSF a Bessell function and the MTF a complex inverse power function.[11] Still others have reported experimental edge traces that suggest that the paper LSF is a simple exponential[13]:

$$LSF(x) = e^{\frac{-2\pi x}{k}}, \tag{3}$$

which corresponds to the MTF of Eq. 4 with m = 2.[11]

$$MTF(\omega) = \frac{1}{1+(k\omega)^m}. \tag{4}$$

If we adopt Eqs. 3 and 4 as models of paper scattering, then we can use the constant k to compare different types of paper. Consideration of a number of reports[3,4,14] suggests that most common papers fall in the range 0.063 < k < 0.63 mm.

Kubelka–Munk Theory

Kubelka–Munk (KM) theory is often used to describe reflectance, R, and transmittance, T, characteristics of scattering materials commonly used in hardcopy imaging.[15] KM theory expresses R and T as functions of four parameters: an absorption coefficient, K, in mm^{-1}; a scattering coefficient, S, in mm^{-1}; the thickness of the material, Z, in mm; and the reflectance, R_g, of the background on which the material is laid:

$$R = \frac{1 - R_g(a - b\cdot\coth(bSZ))}{a - R_g + b\cdot\coth(bSZ)}, \tag{5a}$$

$$T = \frac{b}{a\cdot\sinh(bSZ) + b\cdot\cosh(bSZ)}, \tag{5b}$$

$$a + \frac{S+K}{S}, \tag{5c}$$

$$b = \sqrt{a^2 - 1}, \tag{5d}$$

$$R_\infty = a - b. \tag{5e}$$

Jorgensen[16] reported a correlation between measured values of S and the resolution characteristics of printed halftone images. More recently Oittinen[14] and Engeldrum and Pridham[12] suggested that KM theory may provide a basis for an *a priori* derivation of the PSF, LSF, and MTF of paper, provided one assumes that light scatters homogeneously in all directions in the paper. The MTF derived from KM theory is as follows[12]:

$$MTF(\omega) = A\sum_{i=1}^{\infty} f(i,\omega), \tag{6a}$$

$$A = \ln\left[\frac{1}{1 - R_\infty^2}\right], \tag{6b}$$

$$f(i,\omega) = \frac{R_\infty^{2i}}{i}\left[1 = (2\pi\frac{\omega}{2bSi})^2\right]^{-\frac{3}{2}}. \tag{6c}$$

Values of K and S can be obtained from measurements of reflectance, R, made over a black background (R_g = 0 in Eq. 5a) and reflectance, $R = R_\infty$, made at infinite thickness (approximated by a thick stack of papers). Equations 5a and 5e can then be solved simultaneously to obtain K and S, as shown by Judd and Wyszecki.[17] Table I shows data for a series of paper types included in this study. Included in the table are traditional coated papers (C); noncoated papers, (N); three noncoated, but highly calendered sheets (NCal); two translucent papers manufactured with index-matching resin in the paper furnish (T); and two non-fiber, polymer films (P) manufactured for use in ink-jet printers. The polymer films contain white scattering pigments in the polymer matrix.

Using the values of S and K shown in Table I, MTF functions for each paper were modeled with Eq. 6. Figure 2 shows a plot of Eq. 6 for the K and S values of paper type G. For comparison the empirical model of Eq. 4 is also shown in Fig. 2. A value of k was selected to provide an exact match with Eq. 6 at MTF = 0.5, and a value of m = 1.7 was found to provide an excellent fit between the two MTF functions. It should be noted that the value of k that exactly matches the two functions at MTF = 0.5 is independent of the value of m in Eq. 4.

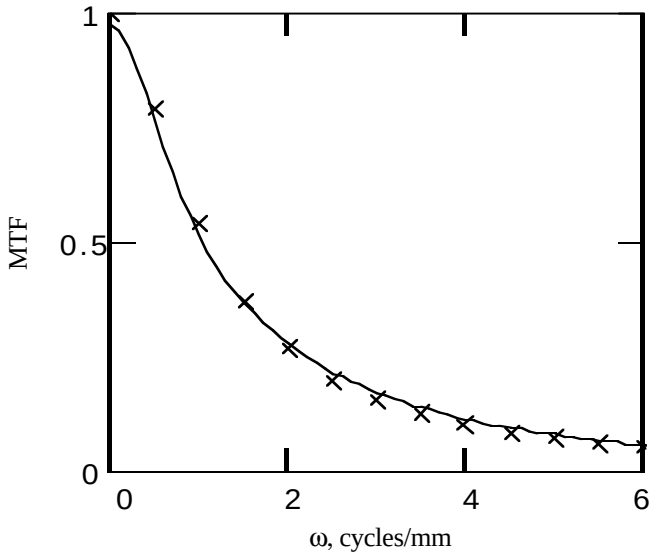

Figure 2. (—) MTF function for paper G derived from Kubelka–Munk theory . (··· x ···) MTF modeled with Eq. 4, k = 0.99 mm and m = 1.7.

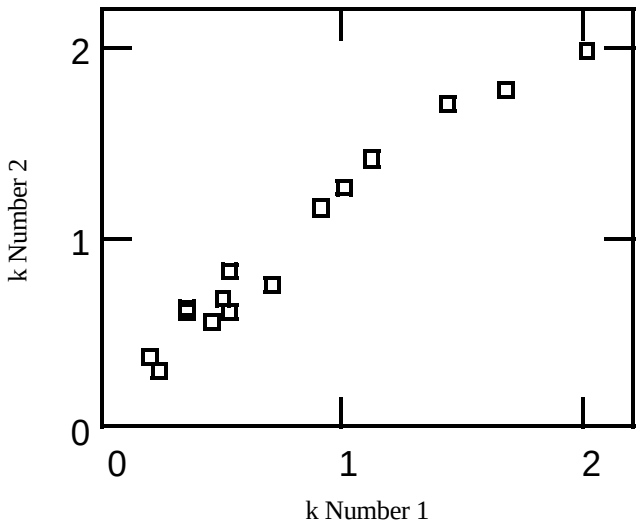

Figure 3. Repeatability test for values of the MTF constant, k, calculated from Kubelka–Munk theory and reflectance measurements. The values of k Numbers 1 and 2 were determined by two different experimentalists.

Values of k corresponding to each combination of K and S in Table I were determined by matching the MTF functions as described above. These values of k are shown in Table I and labeled k_R to distinguish them from other methods of measuring k. The repeatability of this analysis was demonstrated by two sets of measurements of k_R performed independently by two of our authors. Figure 3 shows k_R from one experimenter versus k_R from a second experimenter. Inspection of the data shows that the values of k_R range from about 0.2 to 2.0 mm with an uncertainty on the order of ± 0.15 mm. The values of k_R shown in Table I are the averages of these two determinations.

It is evident from these data that the value of the spread function of paper, k, is governed not only by the scattering coefficient, S, but also by the absorption coefficient, K, of the paper. Intuitively, one would also expect the thickness, Z, and the reflectance of the background, R_g, to impact the lateral spread of light. For example, if the paper were infinitely thin and R_g were black, then light would be absorbed in the background material before it had an opportunity to scatter laterally. Then MTF would be unity with k = 0. Because R_g and Z do not appear in Eq. 6, this is a model for lateral light scatter when the paper is stacked to infinite thickness.

As discussed above, direct measurement of k from microdensitometry line traces of edges is difficult and noisy. Measurement of K and S, on the other hand, is easy and simple to accomplish with readily available reflection spectrophotometers.[17] Thus, it is of considerable interest to examine the utility of KM theory as a method of measuring the lateral scattering characteristics of paper. To do this, independent experimental values of k were extracted from direct measurements of the Yule–Nielsen effect.

Measuring *k* from the Yule–Nielsen Effect

The significance of lateral light scattering is manifested clearly in the Yule–Nielsen effect. Thus, if the Yule–Nielsen

Table I. Summary of Paper Types and Data*

Paper	Type	Z(mm)	S(mm^{-1})	K(mm^{-1})	k_R(mm)	k_p(mm)	k_m(mm)	m
A	NCal	0.084	52.5	0.298	0.46	0.64	0.75	2.00
B	NCal	0.106	43.3	0.237	0.53	0.53	0.63	1.65
C	T	0.076	14.6	0.165	1.11	0.99	1.14	2.00
D	N	0.097	35.4	0.421	0.50	0.53	0.63	1.84
E	P	0.122	5.5	0.238	1.67	1.28	1.68	1.64
F	P	0.089	5.4	0.230	1.43	1.20	1.35	2.00
G	NCal	0.073	7.9	0.227	0.91	0.76	0.71	2.00
H	C	0.056	26.8	0.130	0.25	0.34	0.48	1.16
I	C	0.089	80.9	1.317	0.14	0.25	0.27	1.00
J	N	0.130	79.4	0.597	0.96	0.60	0.59	1.67
K	N	0.124	40.8	0.069	0.65	0.44	0.49	1.42
L	N	0.093	45.1	0.242	0.49	0.60	0.69	1.80
M	N	0.122	47.9	0.675	0.81	0.44	0.46	1.56
N	N	0.092	57.4	0.090	0.89	0.53	0.60	1.74
O	T	0.104	47.2	0.683	2.00	1.86	2.13	2.00

*NCal, noncoated, highly calendered sheet; *T,* sheet rendered translucent by addition of index-matching resin; N, noncoated sheet; C, coated sheet; *Z,* thickness of the sheet in mm; *S* and *K,* Kubelka–Munk scattering and absorption coefficients. The *k* values are MTF constants for Eq. 4 determined from Kubelka–Munk theory (*R*), the line screen technique with m = 1.7 (*p*), and the line screen technique with *m* adjusted for the closest fit (m).

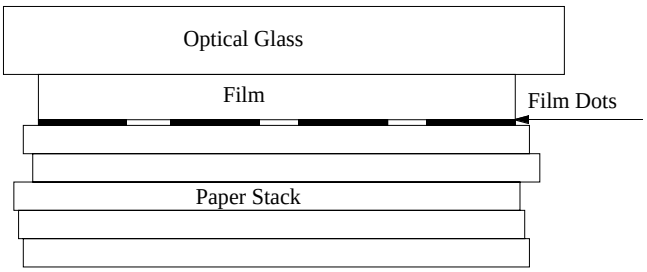

Figure 4. Arrangement of line screen film with stack of paper under analysis.

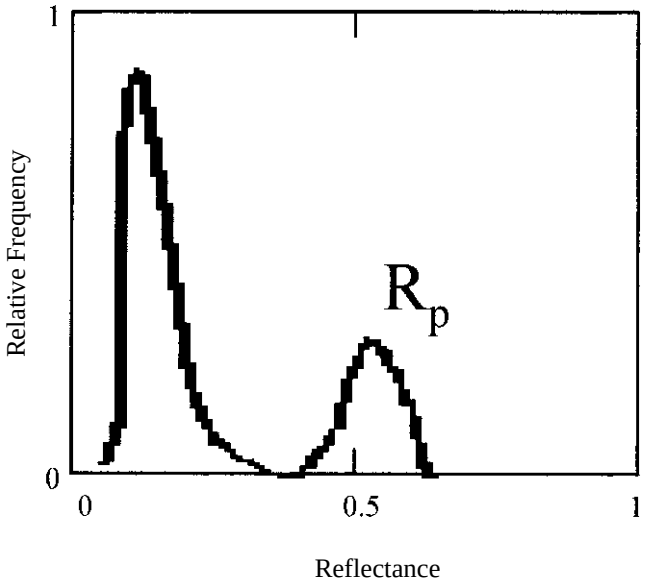

Figure 5. Example of histogram of reflectance values for an image of a line screen on paper. Paper sample G, $F = 0.75$, and $\omega_0 = 1.58$ cycles/mm (40 lPI).

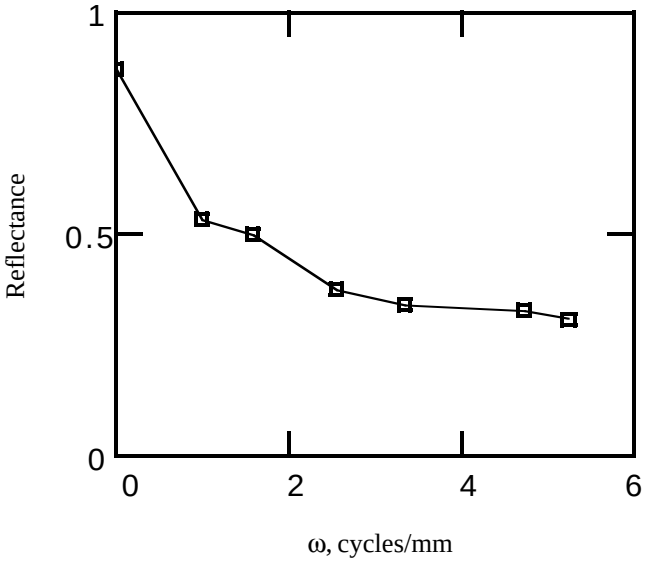

Figure 6. Peak histogram reflectance, R_p, for paper sample G as a function of line screen frequency.

effect can be modeled, it should be possible to extract MTF constants, k, from experimental measurements of the Yule–Nielsen effect. To do this, an idealized halftone system is needed. The ideal halftone in this case is a one-dimensional halftone consisting of linear bar lines rather than dots. High-resolution photographic transparent line screens of this kind are readily available from Beta Screen Corporation (Carlstadt, NJ). Six such screens, each at $F = 0.75$ (75% dot and 25% clear film) and ranging from $\omega_0 = 0.984$ to 5.24 cycles/mm (25 to 133 LPI) were obtained. Each was clamped mechanically in close contact with the paper sample under study, emulsion side down. The paper samples were stacked to approximate an infinite thickness of paper as shown in Fig. 4. The stack was illuminated at 45 degrees, with detection at 0 degrees. Illumination was in line with the direction of the halftone bar lines to minimize any effects of shadow casting from the small, but finite, thickness of the bar lines. Images of the illuminated stack were captured through a microscope with a field of view of 4.0 mm using a COHU Model 4810 CCD camera, PC frame grabber, and software described previously.[18] Pixel values for this system are linear with respect to irradiance at the image plane of the camera and thus are linear with respect to reflectance of the material being imaged. Pixel values in the image were referenced, pixel by pixel, to a known white standard, and the resulting image, in reflectance units, was analyzed to generate the reflectance histogram. Figure 5 shows a typical histogram. From histograms at each value of ω_0 mean values of the reflectance of the paper between the halftone lines, R_p, were obtained. These values were plotted, as shown in Fig. 6 for paper sample G, as a function of ω_0. As shown previously,[19,20] the reflectance of the paper between the dots decreases as F increases and as the screen frequency increases. From this behavior it should be possible to extract a value of k by fitting the data on R_p versus ω_0 to a model containing k. First, however, the impact of the MTF of the instrument must be considered.

To determine the significance of the instrument contribution to the data, the MTF of the camera was measured independently by capturing an image of the edge of an industrial razor blade illuminated from the back. The image of the edge was scanned in software to obtain the LSF characteristic of the instrument. From the LSF the MTF was calculated. The result was an MTF = 0.97 ± 0.03 from 0 to 6 cycles/mm, and MTF = 0.5 at 40 cycles/mm. This corresponds to an instrumental $k = 0.025$ mm, which is an order of magnitude smaller than k values typical of papers. Thus the instrument MTF was assumed to be unity over the range $0 < \omega_0 < 5.24$ cycles/mm over which the experimental line screen data were measured.

To extract a k value from the data shown in Fig. 6 we first derive a model of R_p versus ω_0. We begin with the Fourier series shown in Eq. 7. This function describes the one-

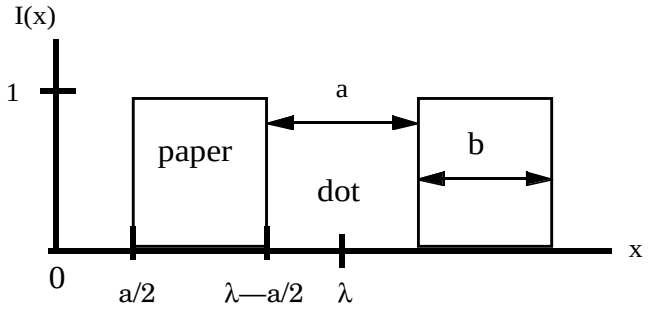

Figure 7. Diagram of periodic square wave pattern described by the Fourier series of Eq. 7. $F = 1 - F_p$, and $\omega = 1/\lambda$. The paper between the dots is width a, and the dot is width b. The edge of the paper begins at $x = a/2$ and ends at $x = \lambda - a/2$.

dimensional square wave function, $I(x)$, of spatial frequency ω_0 shown in Fig. 7.

$$I(x) = F_p + \frac{2}{\pi}\sum_{n=1}^{\infty}\frac{-1^n}{n}\sin(n\pi F_p)\cdot\cos(n2\pi\omega_0 x). \quad (7)$$

This function describes the flux pattern of light that enters the paper after passing the screen lines, since the screen lines have essentially a zero transmittance. Lateral scattering of light within the paper can be modeled by multiplying the cosine function of the Fourier series by the MTF function for the paper. The MTF was modeled with $m = 1.7$ in Eq. 4. The reflectance of the unprinted paper, R_0, is included in the model to account for light absorbed by the paper, and the result is a description of the reflectance of the light from the system.

$$R(x) = R_0\left[F_p + \frac{2}{\pi}\sum_{n=1}^{\infty}\frac{-1^n}{n}\sin(n\pi F_p)\cdot MTF(n\omega_0)\cdot\cos(n2\pi\omega_0 x)\right] \quad (8)$$

If we note that $\lambda = 1/\omega_0$, we can set $x = \lambda/2$ in Eq. 8 and predict the peak reflectance of the paper centered between halftone bar lines. Experimentally, however, it is easier to measure the mean reflectance of the paper, R_p, between the bar lines as the reflectance at the peak of the image histogram. This mean reflectance value averages over all of the paper between all of the halftone lines in the captured image and thus can be measured with good precision. We can model this mean reflectance by integrating Eq. 8 from one edge of a halftone line ($x = a/2$) across the paper to the next edge ($x = \lambda - (a/2)$). The result is Eq. 9.

$$R_p(\omega_0) = R_0F_p\left[\sum_{n=-\infty}^{\infty}\mathrm{sinc}^2(nF_p)\cdot MTF(n\omega_0)\right]. \quad (9)$$

Note that R_p is a function of both the line screen frequency, ω_0 , and the line screen fractional area, $F = 1 - F_p$. It is easy to show that the limiting reflectance of R_p is R_0 at $\omega_0 = 0.0$ cycles/mm and F_pR_0 at $\omega_0 = \infty$ cycles/mm. It is convenient to define a relative contrast function, Eq. 10, and to plot the data as shown in Fig. 8.

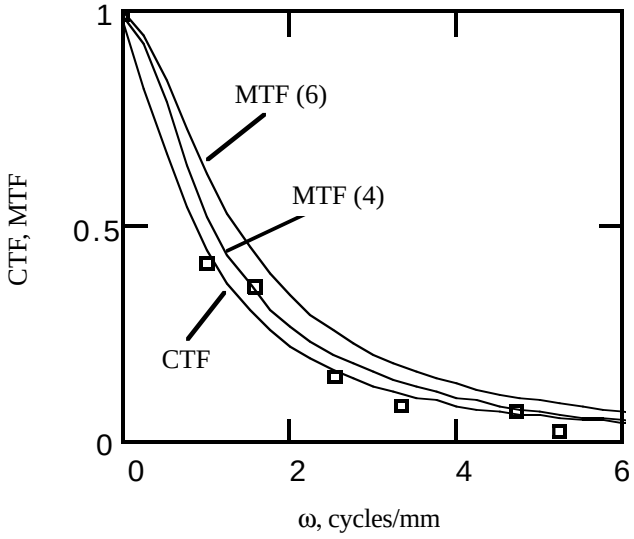

Figure 8. Data (□) are CTF(ω) measured for the noncoated paper G. CTF is Eq. 10 fit to the data. The line marked MTF (4) is Eq. 4 with $m = 1.7$ and the best fit value of k. The line marked MTF (6) is the Kubelka–Munk MTF drawn with experimental values of S and K.

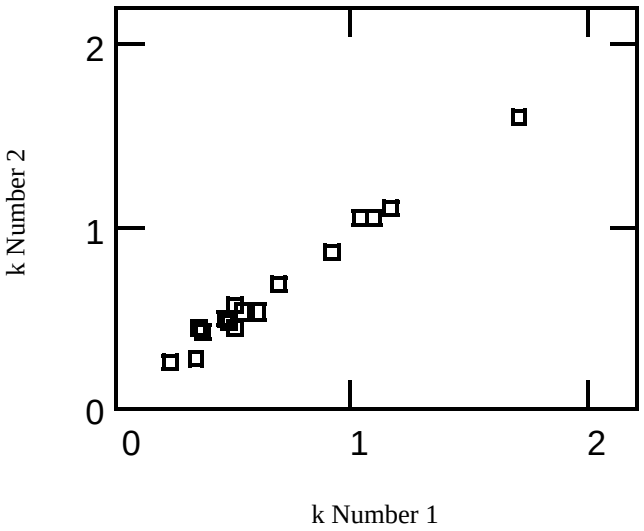

Figure 9. Repeatability test for values of the MTF constant, k, determined by the line screen experiment. The values of k Numbers 1 and 2 were determined by two different experimentalists.

$$CTF(\omega_0) = \frac{R(\omega_0) - R_\infty}{R_0 - R_\infty} \quad (10)$$

We can model the CTF(ω_0) function by starting with an assumed value of k in Eq. 4 and then calculating the $R_p(\omega_0)$ function with Eq. 9, followed by CTF(ω_0) with Eq. 10. The reflectance of the unprinted paper, R_0, is measured independently, and the value of k for the model is selected to provide the minimum rms deviation between the model and the experimental data. The line marked CFT in Fig. 8 is the best fit of the model to the data for paper G. Also shown is the MTF curve of Eq. 4 corresponding to the best fit value of k. For comparison, the MTF from KM theory, Eq. 6, is also shown for the S and K values of paper G in Table I. Values of k determined from line screen data for each paper are listed as k_p in Table I.

The repeatability of the line screen analysis for k_p was demonstrated by two independent sets of measurements of the papers in Table I performed by two of our authors. Figure 9 shows k_p from one experimenter versus k_p from the other experimenter. Inspection of the data shows that the values of k_p range from between 0.2 and 2.0 mm with an uncertainty on the order of ±0.10 mm. All of the k_p values in Table I are the averages of at least two determinations.

A common approximation used in the literature is that the MTF of paper is the same in both the machine and the cross direction of paper. The simplification achieved by this approximation is useful, but common experience with most paper properties suggests that paper is highly directional. To examine the significance of paper directionality with regard to lateral scattering, values of k_p were determined by the line screen method with the lines oriented

Table II. Comparison of Cross Direction (XD) and Machine Direction (MD) Measurements of the MTF Constant, k, in Eq. 4 with $m = 1.7$

		Value of k_p	
Paper	Type	MD	XD
I	C	0.21	0.25
A	NCal	0.51	0.54
J	N	0.37	0.37
L	N	0.36	0.31

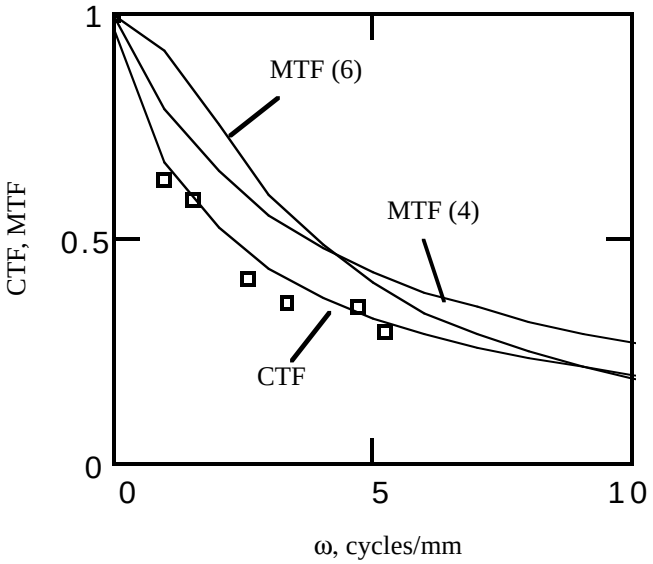

Figure 10. Data (□) are CTF(ω) measured for the coated paper I. CTF is Eq. 10 fit to the data. The line marked MTF (4) is Eq. 4 with m = 1.0 and the best fit value of k. The line marked MTF (6) is the Kubelka–Munk MTF drawn with experimental values of S and K.

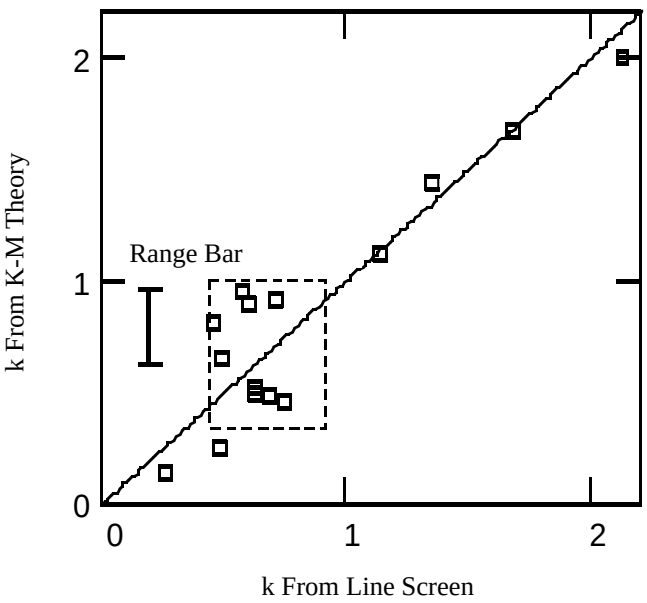

Figure 11. Comparison of MTF k constants determined by Kubelka-Munk theory and reflectance measurements with k constants determined by the line screeen method. The range bar shows the range of k values corresponding to the mottled formation of noncoated paper J. The dotted line shows all of the noncoated and noncoated but calendered sheets.

parallel to the machine direction of the paper. The analysis was repeated with the line screens running perpendicular to the machine direction. The results, summarized in Table II, suggest that the differences in k_p between types of paper is much more significant than differences in k_p due to paper directionality. Indeed, directionality differences are less than the estimated uncertainty for the measure of k_p.

Kubelka–Munk versus Line Screen Data

Paper sample G in Fig. 8 is a noncoated but highly calendered sheet and is reasonably well modeled both by Eq. 4 with m = 1.7 and by Eq. 6. In contrast the coated sheets, H and I, did not fit well with Eq. 4 and m = 1.7. A good fit was achieved with Eq. 4 by varying both m and k for a minimum rms deviation. Figure 10 shows the fit for Paper I with m = 1.0. For comparison the KM model of Eq. 6, with S and K values from Table I, is also shown in Fig. 10, and it is evident that the curve shape predicted by KM theory is not in good agreement with the line screen experiment. Engeldrum and Pridham[12] have suggested that the stratified structure of coated papers is at odds with the assumption of homogeneity in the KM model. Thus it is possible that a value of $m < 1.7$ may be an indication of this inhomogeneity.

All of the paper samples in Table I were modeled using Eq. 4, adjusting both k and the power m. These best fit values of k are listed as k_m in Table I along with the best fit values of m. Inspection of the k_p and k_m values indicates little significant difference between the two, even for the coated sheets, H and I .

The assumption of homogeneous light scattering implied by KM theory was also examined by correlating k_R from KM theory with k_m values determined by the line screen technique, as shown in Fig. 11. Visual inspection of these data suggests that the overall correlation is good for all but the noncoated sheets (J, K, L, M, and N). This would seem to suggest the noncoated sheets may also vary significantly from homogeneous scattering assumed by Kubelka–Munk theory. In contrast, the coated sheets (H and I), which have m values near 1.0, appear to fall reasonably close to the ideal line of slope 1.0 in Fig. 11. However, this is somewhat misleading. The k values for the coated papers are close to the origin, and in fact the numerical values of k_n are almost twice the values of k_R. It would appear, therefore, that the coated sheets are the least homogenous, followed by the noncoated sheets. The behavior of the translucent and polymeric sheets appears to be quite adequately described by the MTF function derived from Kubelka–Munk theory.

Spatial Inhomogeneity

The term *paper formation* is commonly used to refer to the spatial inhomogeneity easily observed in transmitted light as a random mottle pattern. Visual inspection of the papers in Table I on a light table indicated that the greatest degree of mottle was in the noncoated sheets. To estimate the practical impact of paper formation on the Yule–Nielsen effect, paper sample J was examined quantitatively on the light table. With a macroscopic lens and extension tubes on the CCD camera, an image of the paper was captured. The image covered a 2 × 2-cm field of view and clearly displayed the characteristic mottle of paper formation. A reference image of the illuminated, translucent surface of the light table was also captured. The pixels of the paper image were then ratioed, pixel by pixel, with the pixel values of the reference image to obtain transmittance factors, $T(x,y)$. Mean and standard deviations of T = 0.25, σ = 0.028 were determined from these data.

The standard deviation of T indicates a variation in the MTF constant, k, of the paper. To estimate the magnitude of the effect we again use Kubelka–Munk theory. In this case the two equations required to provide values of S and K are Eqs. 5a and 5b for R and T.[17] A mean reflectance R = 0.88 of paper sample J backed by a black surface was measured. Almost no spatial variability in reflectance was observed. With T = 0.25 and R = 0.88 one can solve Eqs. 5a and 5b to obtain mean scattering and absorption coefficients of S = 22.0 mm^{-1} and K = 0.160 mm^{-1}. These in turn lead to an estimate of the mean MTF constant in Eq. 4 of k = 0.909 mm, in reasonable agreement

with the value shown in Table I. If we use the standard deviation of T as an estimator for the range of T values across the sheet, then $(0.25 - 0.028) < T < (0.25 + 0.028)$. Again using KM theory and the mean value of $R = 0.88$ we obtain the range 0.833 mm $< k <$ 1.111 mm for the MTF constant of Eq. 4. This range is illustrated by the range bar shown in Fig. 11.

Discussion

In choosing an experimental method for estimating the MTF characteristics of paper and similar substrates, the edge trace technique (involving a microdensitometry scan of an illuminated knife edge) is the most difficult and least precise. The line screen method, on the other hand, is much easier to perform and can be done with reasonably high precision. Moreover, it provides a measure of the MTF characteristic of paper in a way that is clearly relevant to practical resolution and optical dot gain characteristics of the paper. Reflectance measurements, coupled to Kubelka–Munk theory, are generally easier to perform than the line screen measurements, and instrumentation for reflection measurements is readily available in many laboratories. The Kubelka–Munk description of MTF has the additional advantage of showing the relationship between MTF and the more fundamental metrics of scattering probability, S, and absorption probability, K. However, KM theory appears not to provide as exact an estimate of lateral spread and thus of optical dot gain as can be achieved by the line screen technique.

The papers and substrates used in this study were all manufactured for imaging applications. The two coated sheets are typical sheets for offset lithographic printing, and the noncoated sheets are typical of electrophotographic copy papers and letterhead bond papers. The highly calendered sheets, the translucent sheets, and the polymer films were all manufactured for desktop ink-jet applications. Taken as a group, these papers represent an extreme range of lateral scattering characteristics (0.2 mm $< k <$ 2.0 mm). Over this extreme range, the correlation between k_R from Kubelka–Munk theory and k_m from the line screen experiment appears moderately good. However, this is misleading due to the extreme range of k values involved in the study. Most commonly encountered imaging applications employ papers and substrates over only a fraction of this range. For example, over the commonly encountered range of printing and office copy papers ($0.2 < k < 0.7$ mm) the correlation between KM theory and the line screen experiment is poor.

The reason for the poor showing of Kubelka–Munk theory in this application is not entirely clear. Repeatability experiments shown in Figs. 3 and 9 suggest that the low correlation is not entirely a result of random experimental error. Spatial variability as a result of paper formation might be of a magnitude sufficient to cause the poor correlation shown in Fig. 11. However, reflectance measurements were made over a circular area 2 cm in diameter, which should average the paper formation effect. Whereas the field of view for the line screen measurements was much smaller (4 mm × 4 mm), significant variability due to paper formation would have been expected in Fig. 9. Again, the high correlations seen in Figs. 3 and 9 relative to that seen in Fig. 11 seem to rule out a significant effect due to paper formation.

Another possibility for the poor correlation between KM theory and the line screen experiment is the assumption of homogeneity in light scatter inherent in the KM model. Although direct evidence for inhomogeneous light scatter was not observed when machine and cross-direction line screen measurements were compared, differences between lateral and z direction scattering cannot be ruled out. It is also possible the fundamental scattering process in many papers may not be in accord with Kubelka–Munk theory. KM theory assumes that the rates of change in light flux (dI/dx) from down-moving to up-moving in a sheet, and from up-moving to down-moving (dJ/dx), are both first order with respect to the flux magnitudes, I and J, with an identical proportionality constant, S.[15] None of the data presented in this paper address this assumption, and additional work appears to be warranted to elucidate further scattering mechanisms in the various types of papers used as image substrates.

Acknowledgment. This work was supported by grants from Mead Central Research and 3M Corporation. Special thanks to Bruce Blom, Andrew Virth, and Dick Fisch. Thanks also to Rexham Graphics for supplying experimental paper samples.

References

1. J. A. Stephen Viggiano, *TAGA Proc.*, p. 44 (1990).
2. J. R. Huntsman, *J. Imaging Technol.*, **13**: 136 (1987).
3. M. Maltz, *J. Appl. Photogr. Eng.*, **9**: 83 (1983).
4. J. A. C. Yule, D. J. Howe, and J. H. Altman, *TAPPI*, p. 337 (1967).
5. F. R. Ruckdeschel and O. G. Houser, *Appl. Opt.*, **17**: 3376 (1978).
6. J. A. C. Yule and W. J. Neilsen, *TAGA Proc.*, p. 65 (1951).
7. M. Pearson, *TAGA Proc.*, p. 415 (1980).
8. W. W. Pope, *TAGA Proc.*, p. 415 (1989).
9. J. L. Kofender, Optical spread junctions and noise characteristics of selected paper substrates measured in typocal reflection optical system configurations, *Master's Thesis*, Center for Imaging Science, Rochester Institute of Technology (1987).
10. H. Wakeshima and T. Kunishi, *J. Opt. Soc. Amer.*, **58**: 272 (1968).
11. J. C. Dainty and R. Shaw, *Image Science*, Academic Press, New York, 1974, pp. 244–258.
12. P. G. Engeldrum and B. Pridham, *TAGA Proc.*, **339** (1995).
13. P. Oittinen and H. Saarelma, *Paperi Ja Puu Paper & Timper*, **75**: 66 (1993).
14. P. Oittinen, in *Advances in Printing Science and Technology*, W. H. Banks, Ed, **16**: 121 (1982).
15. G. Wyszecki and W. S. Stiles, *Color Science*, 2nd ed., John Wiley & Sons, New York (1982), p. 221.
16. G. Jorgensen, *GATF Res. Prog.*, **47**: Memo No. 1 (1960).
17. D. B. Judd and G. Wyszecki, *Color in Business, Science and Industry*, J. Wiley & Sons, New York, 1975, pp. 420–438.
18. D. Stewart, R. Sharf, and J. Arney, *J. Imaging Sci. Technol.*, **39**: 261 (1995).
19. J. Arney and H. Zing, *TAGA Proc.*, **353** (1995).
20. P. G. Engeldrum, *J. Imaging Sci. Technol.*, **23**: 545 (1994).